

FLARE ACTIVITIES OF THE CENTRAL ENGINE OF A SUPERLUMINOUS SUPERNOVA

YUN-WEI YU^{1,2} AND SHAO-ZE LI¹*Draft version December 9, 2024*

ABSTRACT

For a recent discovered super-luminous supernova (SLSN) SN 2015bn, some significant undulations appear in its light curve after its first peak, while the basic trends of the underlying light curve can well be explained with a continuous energy injection from the central engine (probably, a spinning-down neutron star). We propose that these unusual undulations are probably caused by some late intermittent pulse energy injections, which indicates that some late energetic flare activities have happened on the central engine of this SLSN. The similarity between the SLSN engines with the central engines of gamma-ray bursts, whose flare activities have been widely confirmed by observations, suggests that these two different phenomena could have some intrinsic connections and even a common astrophysical origin.

Subject headings: gamma-ray burst: general — stars: neutron — supernovae: general

1. INTRODUCTION

Since the late 1990s, a series of modern supernova surveys have discovered an unusual type of supernovae with an absolute magnitude at peak emission of $M_{AB} < -21$ that is more luminous than normal Type I and II supernovae by a factor of $\sim 10-100$ (Ofek et al. 2007; Quimby et al. 2007, 2011; Smith et al. 2007, 2016; Gal-Yam et al. 2009; Chornock et al. 2013; Inserra et al. 2013; Lunnan et al. 2013; Nicholl et al. 2013, 2016; Howell et al. 2013; McCrum et al. 2014; Vreeswijk et al. 2014; Leloudas et al. 2015; Bersten et al. 2016; Dong et al. 2016). The total radiated energy of a typical superluminous supernova (SLSN) is on the order of $\sim 10^{51}$ erg and so far a record of a few times 10^{52} erg has been reached by the most luminous supernova ASASSN-15lh (Dong et al. 2016). If the radiation of these SLSNe is mainly powered as usual by the radioactive chain $^{56}\text{Ni} \rightarrow ^{56}\text{Co} \rightarrow ^{56}\text{Fe}$, then an extremely large amount (several to several tens of solar masses) of radioactive ^{56}Ni would be required. In most cases, this would give a serious challenge to the traditional nucleosynthesis mechanism for supernova explosions (e.g. Umeda & Nomoto 2008).

Gal-Yam (2012) suggested that SLSNe can be divided into three distinct physical subtypes. For the first one denoted by SLSN R, their late-time decay of emission follows the theoretical ^{56}Co decay rate and the peak luminosity is broadly consistent with the corresponding amount of ^{56}Ni . Here the high mass of ^{56}Ni could be produced if these supernova explosions are triggered due to pair-production instability (Woosley et al. 2007; Gal-Yam et al. 2009). These SLSNe R could tend to exist at high redshifts (McCrumb et al. 2014). For another two subtypes termed SLSN I and SLSN II, a powerful central engine is believed to play an essential role in driving explosions and in powering supernova emission, by an impulsive and/or a long-lasting energy injection into explosion-ejected stellar envelope. To be specific, at the

initial time of a supernova explosion, the central engine could impulsively provide a great amount of energy to the supernova ejecta and lead it to have a very high initial velocity corresponding to a kinetic energy on the order of 10^{52} erg. Meanwhile, if this explosion happens in dense, extended circum-stellar material (CSM; e.g., stellar wind and some particular material clusters), then the ejecta can be subsequently heated by the conversion of the kinetic energy through the shock interaction between the ejecta and surrounding material (Smith & McCray 2007; Chevalier & Irwin 2011; Ginzburg & Balberg 2012; Inserra et al. 2016). The resulted supernova can be classified to SLSNe II which usually have a hydrogen-rich spectrum. On the contrary, for a hydrogen-poor SLSN I, shock interaction could be weak and the supernova emission is probably powered directly by a long-lasting central engine. A continuous energy release from the engine could be due to the spin-down of a millisecond neutron star (NS; Woosley et al. 2010; Kasen et al. 2010) or due to the feedback of fallback accretion onto a NS or a black hole (Dexter & Kasen 2013). Nevertheless, the above classification could not be sharply contoured. These different energy sources could coexist in some SLSNe (Wang et al. 2015a; Smith et al. 2016), independent of their spectral types. In any case, a long-lasting central engine could be the most viable and most common energy source for most SLSNe (e.g., Inserra et al. 2013) including some ones classified initially to SLSN II (Inserra et al. 2016) and even SLSN R (Dessart et al. 2012).

During the past few years, a remarkable number of light curves of SLSNe, of both hydrogen-poor and hydrogen-rich, have been successfully explained with a continuous energy injection. In this case, it is convenient to connect the SLSN light curves with the temporal behaviors of central engines. Specifically, a luminosity of simple magnetic dipole radiation of a millisecond NS is usually favored by the broadly smooth light curves (Inserra et al. 2013; Howell et al. 2013; Nicholl et al. 2013, 2015; McCrum et al. 2014; Dai et al. 2016; Bersten et al. 2016). Very recently, Nicholl et al. (2016) presented the multi-wavelength observational results of SN 2015bn,

¹ Institute of Astrophysics, Central China Normal University, Wuhan 430079, China, yuyw@mail.ccnu.edu.cn

² Key Laboratory of Quark and Lepton Physics (Central China Normal University), Ministry of Education, Wuhan 430079, China

where, surprisingly, some significant undulations appear in its light curve during the first ~ 150 days. The dataset they provided is extensive and detailed, which enables us to further constrain and even distinguish different SLSN models. As investigated in Nicholl et al. (2016), the basic profile of the bolometric light curve of SN 2015bn, excluding the undulation components, could in principle be modeled by a scenario of that the fast evolving peak emission is caused by ejecta-CSM interaction, while the late-time slowly-decline emission is dominated by ^{56}Co decays. However, it could still be very difficult (if not impossible) to simultaneously model the light curve undulations by successive collisions of the supernova ejecta with some massive shells that were expelled prior to the supernova explosion, where the structure of progenitor and its mass-loss history must be designed and tuned elaborately. Another possibility they discussed is that this SLSN is powered as usual by a lastingly active central engine, which is on the focus of this letter. In the framework of this model, in our opinion, the light curve undulations of SN 2015bn can naturally be explained by invoking some late flare activities of the central engine, while the underlying smooth light curve is constructed by a continuous energy injection.

2. MODELING SN 2015BN

Following Arnett (1982) and Kasen & Bildsten (2010), the evolution of the internal energy E_{int} of a supernova ejecta can be determined by

$$\frac{dE_{\text{int}}}{dt} = L_{\text{in}} - L_{\text{sn}} - 4\pi R^2 vp, \quad (1)$$

where t is the time, L_{in} is the energy injection rate, L_{sn} is the supernova luminosity, R and $v = dR/dt$ are the radius and speed of supernova ejecta, and p is the pressure that can be related to the internal energy by $p = \frac{1}{3}(E_{\text{int}}/\frac{4}{3}\pi R^3)$. The dynamical evolution of the supernova ejecta is given by $dv/dt = 4\pi R^2 p/M_{\text{ej}}$, where M_{ej} is the total mass of ejecta. Then a supernova light curve can be roughly modeled by the following formula:

$$L_{\text{sn}} = \frac{E_{\text{int}}c}{R\tau} (1 - e^{-\tau}), \quad (2)$$

where c is the speed of light, $\tau = 3\kappa M_{\text{ej}}/4\pi R^2$ is the optical depth, and κ is the opacity.

2.1. The underlying profile of light curve

As usual, we firstly consider that a continuous energy supply for SN 2015bn is provided by a newly-born NS with a spin-down luminosity of

$$L_{\text{in}}(t) = L_{\text{in}}(0) (1 + t/t_{\text{sd}})^{-2}, \quad (3)$$

where the initial luminosity $L_{\text{in}}(0)$ and the spin-down timescale t_{sd} are taken as free parameters when we interpret the basic trends of the light curve. As shown in Figure 1 (see also Figure 19 in Nicholl et al. 2016), the light curve of SN 2015bn can well be profiled by the spinning-down NS model. The excess of the first data could be caused by the NS-driven shock breakout emission (Kasen et al. 2016), while the drop of the last three data is due to the leakage of high-energy photons after the ejecta gradually becomes transparent (Wang et al. 2015b).

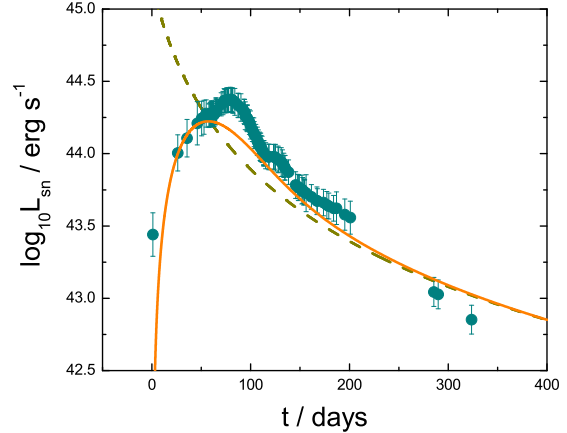


FIG. 1.— A fitting to the underlying profile of light curve of SN 2015b in the spinning-down NS model with parameters $L_{\text{in}}(0) = 1.5 \times 10^{45} \text{ erg s}^{-1}$ and $t_{\text{sd}} = 30 \text{ day}$ (solid line). The dashed line represents the energy injection rate. The parameters for the supernova ejecta are adopted to $\kappa = 0.2 \text{ cm}^2 \text{ g}^{-1}$, $M_{\text{ej}} = 5M_{\odot}$, and initial velocity $v(0) = 7.5 \times 10^8 \text{ cm s}^{-1}$.

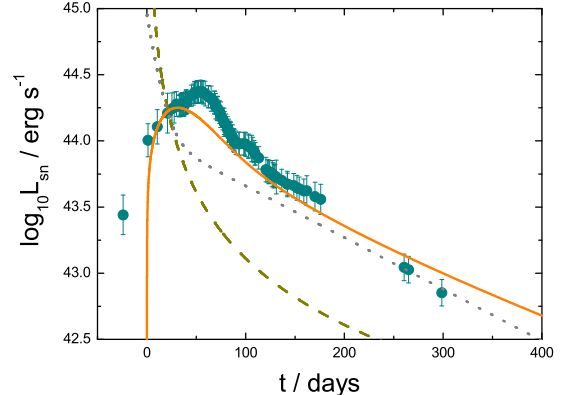


FIG. 2.— An example fitting to the underlying profile of light curve of SN 2015b by combining the heating effects due to fallback accretion and radioactive decays of ^{56}Ni (Solid line). The energy injection rates due to fallback accretion and radioactivity are presented by the dashed and dotted lines, respectively. The model parameters are taken as $L_{\text{in}}(0) = 4.7 \times 10^{49} \text{ erg s}^{-1}$, $t_{\text{accr}} = 1000 \text{ s}$, $\kappa = 0.2 \text{ cm}^2 \text{ g}^{-1}$, $M = 10M_{\odot}$, $v(0) = 5 \times 10^8 \text{ cm s}^{-1}$ and $M_{\text{Ni}} = 8M_{\odot}$.

Secondly, a continuous energy supply could also come from an outflow that is driven as the feedback (e.g. disk wind) of a fallback accretion onto the central compact object (a NS or a black hole). By assuming a direct proportion to the accretion rate, the outflow luminosity due to the fallback accretion can be written as (Piro & Ott 2011)

$$L_{\text{in}}(t) = L_{\text{in}}(0) \left[(t/t_{\text{accr}})^{-1/2} + (t/t_{\text{accr}})^{5/3} \right]^{-1}. \quad (4)$$

Here the accretion timescale t_{accr} can roughly be estimated by a free-fall timescale of $\sim (G\rho_0)^{-1/2}$ (Dexter & Kasen 2013), which gives a typical value of a few hundreds to a thousand of seconds for a typical stellar density of $\rho_0 \sim 300 \text{ g cm}^{-3}$. During such a short time, the

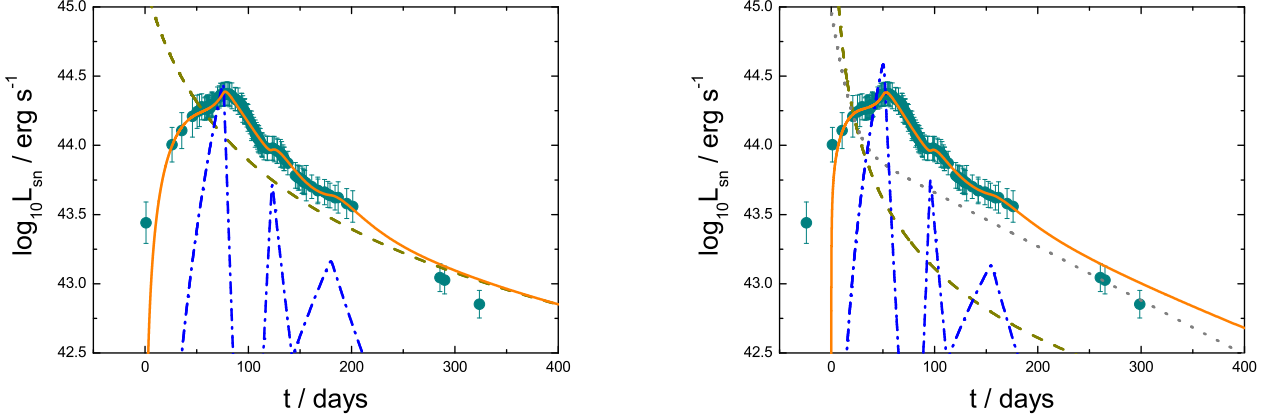


FIG. 3.— Fittings to the light curve of SN 2015bn (solid lines) in the spinning-down NS model (left panel) and the fallback accretion model (right panel). For modeling the undulations, three flaring intermittent energy injections are invoked (dash-dotted lines). The parameters for the continuous energy injections are the same to Figure 1 and Figure 2.

most extractable energy of the fallback material has been released and injected into the supernova ejecta. As a result, on one hand, the light curve is predicted to decrease too quickly after the peak to be consistent with the observational data, if an appropriate ejecta mass is taken to fit the light curve peak. In order to improve the fitting to the late emission, we additionally introduce an artificial mass of $8M_{\odot}$ of radioactive ^{56}Ni . Then, as shown in Figure 2, an example fitting to the underlying profile of the light curve can be obtained by combining the heating effects due to fallback accretion and radioactive decays of ^{56}Ni . However, here an extremely high (probably unpractical) efficiency of nickel production of about 80% is indicated by comparing the nickel mass to the total ejecta mass ($10M_{\odot}$) that is determined by the peak-emission time. It should be noticed that the pair-instability supernova model can not be employed here because of the presence of the central compact object. On the other hand, the early-injected energy should mostly be converted into the kinetic energy of the ejecta very quickly, which determines a high velocity of about $3 \times 10^9 \text{ cm s}^{-1}$. This velocity is several times higher than the observed photosphere velocity of SN 2015bn of $\sim 9 \times 10^8 \text{ cm s}^{-1}$ (Nicholl et al. 2016), which further disfavors the fallback accretion model, although a precise calculation of photosphere velocity is dependent on the specific matter distributions of the ejecta.

To be summarized, in principle, the above two models of a lastingly active central engine can both give a plausible explanation for the underlying profile of the light curve of SN 2015bn. In comparison, the simple spinning-down NS model could be much more favored.

2.2. Light curve undulations and flare activities

A lastingly active central engine actually has been widely suggested to account for many features of afterglow emissions of gamma-ray bursts (GRBs). On one hand, a continuous energy release, usually from a millisecond magnetar, was always employed to explain the shallow-decay or plateau afterglows of GRBs (Dai & Lu 1998a,b; Zhang & Meszaros 2001; Yu et al. 2010; Rowlinson et al. 2013; Lü et al. 2015). On the other hand, more interestingly, a great number of rapidly rising and de-

clining X-ray flares have been widely discovered in about one-third of Swift GRBs (Burrows et al. 2005; Falcone et al. 2007; Chincarini et al. 2007; Wang & Dai 2013; Yi et al. 2016). This robustly indicates that many intermittent and energetic activities have taken place on the GRB engines and, furthermore, leads us to consider that the central engines of SLSNe may also be able to generate some similar flare activities. As a natural result, some undulations like in the light curve of SN 2015bn could be caused by such delayed flaring energy releases.

For an empirical fitting to the light curve of SN 2015bn, we describe the energy release rate due to an engine flare by the following formula

$$L_{\text{flare}}(t) = L_{\text{flare,p}} \left[\left(\frac{t}{t_{\text{flare,p}}} \right)^{\alpha_1 w} + \left(\frac{t}{t_{\text{flare,p}}} \right)^{\alpha_2 w} \right]^{-1/w}, \quad (5)$$

which was usually adopted to fit the light curves of GRB X-ray flares, where the structure parameters α_1 , α_2 , and w reflect the sharpness and smoothness of the flares. By assuming a possible universal nature of flare activities, we take values of the structure parameters referring to the fitting results of GRB flares (Yi et al. 2016). Nevertheless, different from the GRB situations with optically-thin ejecta, here we cannot use Equation (5) to directly confront with supernova light curves, because the flare energies would be completely absorbed by the optically-thick supernova ejecta and influence the supernova emission as some intermittent energy injections. Therefore, the consequent supernova light curves are primarily related to the parameters $L_{\text{flare,p}}$ and $t_{\text{flare,p}}$, but insensitive to the structure parameters. By substituting expression (5) into Equation (1), we attempt to fit the light curve undulations of SN 2015bn with flare activities. A perfect result is shown in Figure 3 (left Panel), where three obvious flares are invoked. Besides the spinning-down NS model, the less likely fallback accretion model is still calculated and presented (right panel), just for a general and conservative consideration.

We compare the three SLSN flares with 200 GRB X-ray flares (Wang & Dai 2015; Yi et al. 2016) in the $L_{\text{flare,p}} - t_{\text{flare,p}}$ plane in Figure 4. As shown, the three SLSN flares can basically satisfy the extension of the

correlation determined by the GRB flares. This implies that the central engines of GRBs and SLSNe could indeed have a common nature. The statistics of GRB flares shows that central engines are usually more active at earlier time. Therefore, one may query that why we have never yet detected any signature for the more frequent early flares from so many observed SLSNe, except for the present three late flares. On one hand, observational data during the increasing phase of a supernova is indeed usually too sparse to exhibit the details of light curve. On the other hand, more intrinsically, even though the temporal evolutions of flares are very sharp, their consequent undulations in supernova light curves are actually gentle because of the trapping of photons in the ejecta before the ejecta becomes completely transparent. The earlier the time, the more serious the trapping effect. As a result, any fluctuation in an energy injection history can basically be smoothed in the consequent light curve, in particular, before the photon diffusion timescale. In other words, it is nearly impossible to detect any obvious flare signature from a supernova light curve before its peak, no matter how many flares have happened then.

Although the above empirical fittings demonstrates the availability of the flare explanation for the light curve undulations of SN 2015bn, it is still unclear what the nature of these engine activities are. In the most favorable spinning-down NS model, one may firstly recall the GRB flare model due to magnetic reconnections that happen on NS surface after intense magnetic fields float from stellar interior (Dai et al. 2006). Specifically, in the case of SN 2015bn, the dipolar magnetic field strength and initial spin period of the NS can be derived to $B_p = 6.4 \times 10^{13}$ G and $P(0) = 2.3$ ms from the expressions of spin-down luminosity $L_{\text{in}}(0) = 10^7 B_p^2 P(0)^{-4} \text{erg s}^{-1}$ and timescale $t_{\text{sd}} = 2 \times 10^{39} B_p^{-2} P(0)^2$ s. This dipolar field is not very high but just comparable to the fields of some normal Galactic pulsars, which could challenge the magnetic reconnection origin of the flares. However, it cannot be ruled out that the NS could have much higher multipolar internal magnetic fields, which is at least supported by the discovery of some so-called low-field magnetars in our galaxy (e.g. Rea et al. 2010). In any case, the magnetic configuration of the NS must be described carefully in order to account for the flare properties, in particular, for the very late reconnection occurrence time of $\sim 10^7$ s. As an alternative choice, the flare activities could also be caused by accreting some separated clusters of material (Perna et al. 2006; Proga & Zhang 2006), although a continuous accretion is disfavored by the basic trends of the light curve of SN 2015bn.

3. DISCUSSIONS ON GRB-SLSN CONNECTION

The continuity between the flare properties of SLSNe and GRBs indicates that these two different phenomena could have an intrinsic connection and even a common origin. A very competitive scenario is that both GRBs and SLSNe are produced as outcomes of the formation of a millisecond NS from core-collapse of a massive rapidly rotating progenitor star. A rough difference is that, the rotational energy of the NSs can be extracted during a short timescale for GRBs, whereas for most SLSNe the energy is released slowly through magnetic dipole radiation. We suspect that the most critical factors deter-

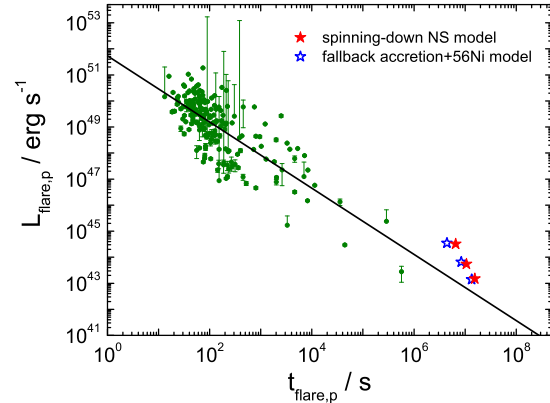


FIG. 4.— A comparison of the flares of SN 2015bn (stars) with 200 GRB flares (solid circles) in the peak luminosity-peak time plane. The solid line presents the correlation between the peak luminosities and peak times of GRB flares.

mining this difference could be the strength of dipolar magnetic fields and the amount of fallback material.

The dipolar magnetic field of a NS harbored in a GRB could be statistically much higher than those of SLSN NSs (Rowlinson et al. 2013; Lü et al. 2015), which makes the fallback accretion onto the NS easily to trigger a propeller process. As a result, on one hand, the rotational energy of the NS can be extracted quickly, effectively, and nearly isotropically by a propeller outflow, which pushes and accelerates the supernova ejecta to a very high speed (Piro & Ott 2011). On the other hand, the coupling of the outflow with the strong magnetic fields on the direction of magnetic axis could collimate a certain fraction of outflow energy to form a relativistic GRB jet. After the propeller phase, the NS can further release energy through magnetic dipole radiation, which is relatively longer and weaker than the propeller effect. This continuous energy release could contribute to a plateau afterglow of the GRB but has little influence on the supernova luminosity, because the spin-down timescale is still much shorter than the photon diffusion time of the supernova ejecta and the magnetic dipole radiation could be collimated due to the high field. Therefore, the emission of a GRB-associated supernova (hypernova) is usually broad-lined due to the high speed but primarily powered by radioactive decays of ^{56}Ni (Cano et al. 2016). Here we want to emphasize that, although the GRB jet is collimated within a small cone, the energy release of the central engine during GRB and flare emissions could be in all directions with a specific angle distribution. Therefore, when Figure 4 was plotted above, we simply neglected a possible beaming correction for the luminosities of GRB flares.

For a NS with a relatively low magnetic field, it could be difficult to generate a relativistic GRB jet and drive a propeller outflow. Nevertheless, a small fraction of the gravitational energy of fallback material can still be released through some feedback mechanisms (e.g. disk wind). If the fallback material is abundant enough, the supernova ejecta can be accelerated to a sufficiently high speed to cause energetic shock interaction with CSM. In this case, the NS could quickly collapse into a black hole. In contrast, for an insignificant fallback accretion,

the rotational energy of the NS would be released slowly, nearly isotropically, and totally through magnetic dipole radiation, with a timescale comparable to the ejecta diffusion timescale. As a result, the supernova emission is powered directly and continuously by this lasting energy release. The amounts of fallback material and CSM even may have some correlation.

In any case, a comprehensive statistics of SLSN and GRB parameters will be critical and helpful for testing and constraining some candidate scenarios for a united picture of these two phenomena, as tentatively discussed above. In addition, some bridge samples, such as the recent discovered ultra-long GRB 111209A that is associated with a SLSN (Greiner et al. 2015; Gao et al. 2016), may provide an important clue to the connection between these two phenomena.

4. CONCLUSION

The discovery of the light curve undulations of SN 2015bn, which is very fortunate, may indicate that some late but significant flare activities have taken place on its central engine, as a natural and plausible explanation,

although a more elaborate model description must be required for consolidating and distinguishing this explanation from the others (e.g., the CSM interaction model). By considering of the late times of the flares, we suspect that flare activities of SLSN engines could be as ubiquitous as GRB flares, because the engines are probably more active at earlier time although the early flares are completely smoothed and hidden in supernova light curves. The possible universal law appearing in the flare properties of both SLSNe and GRBs further indicates these two phenomena could have an intrinsic connection and even an united origin, which is worth trying to be revealed and modeled in future.

The Authors thank M. Nicholl and F. Y. Wang for sharing the data of SN 2015bn and GRB flares, respectively. This work is supported by the National Basic Research Program of China (973 Program, grant 2014CB845800), the National Natural Science Foundation of China (grant No. 11473008), and the Program for New Century Excellent Talents in University (grant No. NCET-13-0822).

REFERENCES

Arnett, W. D. 1982, *ApJ*, 253, 785
 Bersten, M. C., Benvenuto, O. G., Orellana, M., & Nomoto, K. 2016, *ApJ*, 817, L8
 Burrows, D. N., Romano, P., Falcone, A., et al. 2005, *Science*, 309, 1833
 Cano, Z., Johansson Andreas, K. G., & Maeda, K. 2016, *MNRAS*, 457, 2761
 Chevalier, R. A., & Irwin, C. M. 2011, *ApJ*, 729, L6
 Chincarini, G., Moretti, A., Romano, P., et al. 2007, *ApJ*, 671, 1903
 Chornock, R., Berger, E., Rest, A., et al. 2013, *ApJ*, 767, 162
 Dai, Z. G. 2004, *ApJ*, 606, 1000
 Dai, Z. G., & Lu, T. 1998, *Physical Review Letters*, 81, 4301
 Dai, Z. G., & Lu, T. 1998, *A&A*, 333, L87
 Dai, Z. G., Wang, S. Q., Wang, J. S., Wang, L. J., & Yu, Y. W. 2016, *ApJ*, 817, 132
 Dai, Z. G., Wang, X. Y., Wu, X. F., & Zhang, B. 2006, *Science*, 311, 1127
 Dessart, L., Hillier, D. J., Waldman, R., Livne, E., & Blondin, S. 2012, *MNRAS*, 426, L76
 Dexter, J., & Kasen, D. 2013, *ApJ*, 772, 30
 Dong, S., Shappee, B. J., Prieto, J. L., et al. 2016, *Science*, 351, 257
 Falcone, A. D., Morris, D., Racusin, J., et al. 2007, *ApJ*, 671, 1921
 Gal-Yam, A., Mazzali, P., Ofek, E. O., et al. 2009, *Nature*, 462, 624
 Gal-Yam, A. 2012, *Science*, 337, 927
 Gao, H., Lei, W.-H., You, Z.-Q., & Xie, W. 2016, *arXiv:1605.04660*
 Ginzburg, S., & Balberg, S. 2012, *ApJ*, 757, 178
 Greiner, J., Mazzali, P. A., Kann, D. A., et al. 2015, *Nature*, 523, 189
 Howell, D. A., Kasen, D., Lidman, C., et al. 2013, *ApJ*, 779, 98
 Inserra, C., Smartt, S. J., Gall, E. E. E., et al. 2016, *arXiv:1604.01226*
 Inserra, C., Smartt, S. J., Jerkstrand, A., et al. 2013, *ApJ*, 770, 128
 Kasen, D., & Bildsten, L. 2010, *ApJ*, 717, 245
 Kasen, D., Metzger, B. D., & Bildsten, L. 2016, *ApJ*, 821, 36
 Lunman, R., Chornock, R., Berger, E., et al. 2013, *ApJ*, 771, 97
 Lü, H.-J., Zhang, B., Lei, W.-H., Li, Y., & Lasky, P. D. 2015, *ApJ*, 805, 89
 McCrum, M., Smartt, S. J., Kotak, R., et al. 2014, *MNRAS*, 437, 656
 Nicholl, M., Berger, E., Smartt, S. J., et al. 2016, *arXiv:1603.04748*
 Nicholl, M., Smartt, S. J., Jerkstrand, A., et al. 2013, *Nature*, 502, 346
 Ofek, E. O., Cameron, P. B., Kasliwal, M. M., et al. 2007, *ApJ*, 659, L13
 Perna, R., Armitage, P. J., & Zhang, B. 2006, *ApJ*, 636, L29
 Piro, A. L., & Ott, C. D. 2011, *ApJ*, 736, 108
 Quimby, R. M., Kulkarni, S. R., Kasliwal, M. M., et al. 2011, *Nature*, 474, 487
 Quimby, R. M., Aldering, G., Wheeler, J. C., et al. 2007, *ApJ*, 668, L99
 Rea, N., Esposito, P., Turolla, R., et al. 2010, *Science*, 330, 944
 Rowlinson, A., O'Brien, P. T., Metzger, B. D., Tanvir, N. R., & Levan, A. J. 2013, *MNRAS*, 430, 1061
 Smith, M., Sullivan, M., D'Andrea, C. B., et al. 2016, *ApJ*, 818, L8
 Smith, N., & McCray, R. 2007, *ApJ*, 671, L17
 Umeda, H., & Nomoto, K. 2008, *ApJ*, 673, 1014-1022
 Vreeswijk, P. M., Savaglio, S., Gal-Yam, A., et al. 2014, *ApJ*, 797, 24
 Wang, F. Y., & Dai, Z. G. 2013, *Nature Physics*, 9, 465
 Wang, S. Q., Liu, L. D., Dai, Z. G., Wang, L. J., & Wu, X. F. 2015a, *arXiv:1509.05543*
 Wang, S. Q., Wang, L. J., Dai, Z. G., & Wu, X. F. 2015b, *ApJ*, 799, 107
 Woosley, S. E. 2010, *ApJ*, 719, L204
 Woosley, S. E., Blinnikov, S., & Heger, A. 2007, *Nature*, 450, 390
 Yi, S.-X., Xi, S.-Q., Yu, H., et al. 2016, *arXiv:1603.07429*
 Yu, Y.-W., Cheng, K. S., & Cao, X.-F. 2010, *ApJ*, 715, 477
 Zhang, B., & Mészáros, P. 2001, *ApJ*, 552, L35